Effects of the magnetic moment interaction between nucleons on observables in the 3N continuum

H. Witała, J. Golak, and R. Skibiński

Insitute of Physics, Jagiellonian University, Reymonta 4, PL-30059 Kraków, Poland

C. R. Howell and W. Tornow

Physics Department, Duke University, Durham, North Carolina 27708, USA
and Triangle Universities Nuclear Laboratory, Durham, North Carolina 27708, USA

The influence of the magnetic moment interaction of nucleons on nucleon-deuteron elastic scattering and breakup cross sections and on elastic scattering polarization observables has been studied. Among the numerous elastic scattering observables only the vector analyzing powers were found to show a significant effect, and of opposite sign for the proton-deuteron and neutron-deuteron systems. This finding results in an even larger discrepancy than the one previously established between neutron-deuteron data and theoretical calculations. For the breakup reaction the largest effect was found for the final-state-interaction cross sections. The consequences of this observation on previous determinations of the $^1S_0$ scattering lengths from breakup data are discussed.

PACS number(s): 21.60.Cs, 25.40.Kv, 27.30.+t

I. INTRODUCTION

The study of three-nucleon ($3N$) bound states and reactions in the $3N$ continuum has improved significantly our knowledge of the nuclear Hamiltonian [1,2]. The underbinding of the triton and ^{3}He nuclei by modern nucleon-nucleon (NN) interactions was the first evidence for the necessity of including three-nucleon forces (3NF) [2] in addition to the pairwise NN interactions. Furthermore, results of Green function Monte Carlo calculations [3] showed that the energy levels of light nuclei can be explained only when the pairwise NN interactions are supplemented by appropriate 3NF's. Additional evidence for 3NF effects came from the study of the cross-section minimum [4] in elastic nucleon-deuteron (Nd) scattering and the deuteron vector analyzing powers [5–7].

Despite the spectacular successes obtained in interpreting $3N$ data based on the concept of a $3N$ Hamiltonian with free NN interactions and supplemented by 3NF's, some dramatic discrepancies remain between theory and data that require further investigation. These discrepancies can be divided into two categories according to energy. One was discovered at incident nucleon lab energies in the $3N$ system above 100 MeV and is exemplified by the nucleon-vector [6,8,9] and deuteron-tensor analyzing powers [5,10] in Nd elastic scattering. Since the 3NF effects become more important with increasing energy [10,11], these discrepancies will play an important role in establishing the proper spin-isospin structure of the 3NF. The second category was found at lab energies below 40 MeV. In the following we will focus on these low-energy discrepancies.

The most famous is the vector analyzing power in Nd elastic scattering. The theoretical predictions based on modern NN interactions, and including 3NF models, underestimate considerably the maximum of the nucleon analyzing power $A_y(\theta)$ in $\vec{p}$-d and $\vec{n}$-d scattering, as well as the maximum of the deuteron vector analyzing power $iT_{11}(\theta)$ in $\vec{d}$-p scattering [10,12,13]. At low energies (up to ≈ 30 MeV)

these two observables are very sensitive to changes in the ^3P_j NN and/or in ^4P_J Nd phase shifts [14,15]. Even very small changes of these phase shifts result in significant variations of $A_y(\theta)$ and $iT_{11}(\theta)$.

Furthermore, low-energy neutron-deuteron (nd) breakup cross sections show clear discrepancies between theory and data [1,16–23] for some special kinematical arrangements of the outgoing three nucleons. The most spectacular ones are the symmetrical space-star (SST) and the quasifree scattering (QFS) configurations.

In the SST configuration the three nucleons emerge in the center-of-mass(c.m.) system in a plane perpendicular to the incoming beam with momenta of equal magnitudes and directed such that the angle between adjacent particle momentum vectors is 120°. The low-energy nd SST cross sections are clearly underestimated by theoretical predictions [16–21]. The calculated cross sections are insensitive to the NN potential used in the calculations [1,11]. They also do not change when any one of the present-day 3NF models is included [1,11].

The QFS refers to the situation where one of the nucleons is at rest in the laboratory system. In nd breakup, np or nn can form a quasifree scattered pair. Both cases have been measured [22,23]. The picture resembles that for SST: the theoretical QFS cross sections are practically independent of the NN potential used in calculations, and they do not change when 3NF's are included [1,11]. The calculated QFS scattering cross section follows nicely the data when np is the quasifree interacting pair [23]. However, when the nn pair is quasifree scattered instead of np, the theory clearly underestimates the experimental cross sections [22,23], similarly to the nd SST case.

A problem of a different kind arises in the nd breakup final-state-interaction (FSI) configuration where the two outgoing nucleons have equal momenta. The cross section for this geometry is characterized by a pronounced peak when the relative energy of the final-state interacting pair reaches zero (exact FSI condition). Due to the large sensitivity of this

enhancement to the $^1S_0$ NN scattering lengths, the FSI geometry has recently been studied in nd breakup with the aim of determining the nn $^1S_0$ scattering length [24,25]. The np FSI cross-section measurements performed simultaneously in Ref. [24] and in two consecutive experiments in Refs. [25,26] seem to indicate that, indeed, this configuration is a reliable tool for determining the NN $^1S_0$ scattering length: the values obtained for a_{np} agreed with the result known from free np scattering [27]. However, the values obtained for a_{nn} in Refs. [24,25] are in striking disagreement with each other, with the result of Ref. [24] in excellent agreement with the accepted value for a_{nn}.

All previously published $3N$ continuum Faddeev calculations for the nd system were restricted to pure strong nuclear forces, while for the pd system the Coulomb interaction between the two protons had been included in addition to the nuclear force [13]. However, the rigorous inclusion of the Coulomb interaction is currently limited to elastic scattering. More subtle electromagnetic contributions, such as the magnetic moment interaction (MMI) between the nucleons have been neglected in exact Faddeev calculations for the $3N$ continuum. The approximate calculation by Stoks [28] at $E_N = 3$ MeV, based on a quasi-two-body approach represents only the leading term of a genuine $3N$ calculation. Since this calculation predicted only a tiny effect on $A_y(\theta)$ in the region of the maximum, it was generally concluded that the exact treatment of the MMI was not worth the effort. However, the speculative interpretation [32] of new data for nd scattering at very low energies and the associated comparison to pd scattering suggested that the MMI is indeed an important ingredient in the $3N$ continuum.

It is the aim of the present paper to go beyond the approximate calculation referred to above and to study extensively the effects of the MMI on Nd elastic scattering and breakup observables using the Faddeev approach. Even though it is very unlikely that such subtle effects will have any significant influence on the QFS and SST cross sections, we found it worthwhile to calculate the magnitude of the MMI effects for these configurations. In Sec. II we present the basic theoretical ingredients of our $3N$ calculations together with a short description of the nucleon magnetic moment interactions. The results for elastic scattering and breakup observables are presented and discussed in Secs. III and IV, respectively. In the breakup section we also focus on the consequences of the MMI effects on the extraction of the $^1S_0$ scattering lengths from nd breakup data. Specifically, we present corrections induced by the MMI on the values for a_{np} and a_{nn} deduced from very recent measurements. We summarize and conclude in Sec. V.

II. THEORETICAL FORMALISM

The transition amplitudes for Nd elastic scattering $\langle \Phi'|U|\Phi\rangle$, and breakup $\langle \Phi_0|U_0|\Phi\rangle$ can be expressed in terms of the vector $T|\Phi\rangle$, which fulfills the $3N$ Faddeev equation [1],

$$T|\Phi\rangle = tP|\Phi\rangle + tPG_0T|\Phi\rangle, \quad (1)$$

as

$$\langle \Phi'|U|\Phi\rangle = \langle \Phi'|PG_0^{-1} + PT|\Phi\rangle,$$

$$\langle \Phi_0|U_0|\Phi\rangle = \langle \Phi_0|(1+P)T|\Phi\rangle. \quad (2)$$

The incoming state $|\Phi\rangle = |\vec{q}_0, \phi_d\rangle$ is composed of the deuteron wave function ϕ_d and the momentum eigenstate $|\vec{q}_0\rangle$ of the relative nucleon-deuteron motion. For elastic scattering the outgoing relative momentum changes its direction leading to a state $|\Phi'\rangle$, while for the breakup reaction the final state $|\Phi_0\rangle$ is a momentum eigenstate that describes the final motion of three outgoing nucleons. The permutation operator P takes into account the identity of nucleons and it is the sum of a cyclic and anticyclic permutation of three particles. The exchange term PG_0^{-1} (G_0 denotes the free $3N$ propagator) in the elastic scattering amplitude results from the interchange of the incoming nucleon with those in the deuteron. All final-state interactions between the outgoing nucleons, driven by a two-nucleon off-shell transition-matrix that is denoted as t in Eqs. (1) and (2), are comprised in the T operator, as can be easily seen by iterating Eq. (1).

This formulation for nucleon-deuteron scattering assumes pairwise interactions between nucleons via a short-range force V, which generates through the Lippmann-Schwinger equation the transition-matrix t. Therefore, it excludes the treatment of the long-range Coulomb force, but allows for the inclusion of any electromagnetic contribution of short-range character, such as, e.g., MMI's between nucleons. In the case of our "pd calculations," the value of the magnetic moment of the two neutrons in our nd breakup calculations is replaced by the value of the proton magnetic moment, i.e., the long-range Coulomb force is not included, neither is any interference between the Coulomb force and the MMI.

In our approach we solve Eq. (1) in momentum space and partial wave basis using the magnitudes of the standard Jacobi momenta $p = |\vec{p}|$ and $q = |\vec{q}|$ to describe the relative motion of the three nucleons, supplemented by angular momenta, spin, and isospin quantum numbers. Due to the short-range assumption, the result is a finite set of coupled integral equations in two continuous variables, p and q. The equations are solved for the amplitudes $\langle pq\alpha|T|\Phi\rangle$ for each total angular momentum J and parity of the $3N$ system by generating the Neumann series of Eq. (1) and summing it up by the Pade method. The $|\alpha\rangle$ is a set of angular, spin, and isospin quantum numbers $|\alpha\rangle \equiv |(ls)j(\lambda 1/2)I(jI)J(t1/2)T\rangle$, which describes the coupling of the two-nucleon subsystem and the third nucleon to the total angular momentum J and total isospin T of the $3N$ system. For details of the theoretical formalism and numerical performance we refer to Ref. [1].

To study effects of the MMI's of the nucleons we included in addition to the strong AV18 [29] or CD Bonn [30] potentials the interactions of the magnetic moments in the pp, np, and nn subsystems. The form and parametrization of the MMI's are given in Eqs. (8), (15), and (16) of Ref. [29] (in the case of the np system the term $\vec{L} \cdot \vec{A}$ in Eq. (15) of Ref. [29] was neglected).

The difference of the pp (nn) and np interactions in isospin $t=1$ states induces transitions between $3N$ states with total isospin $T=1/2$ and $T=3/2$. The strength of these transitions is determined through the known charge-independence breaking of the NN interactions [31]. This charge-independence breaking can be treated approximately by a simple "$\frac{2}{3}$-$\frac{1}{3}$ rule," for which the effective $t=1$ transition matrix is given by $t=2/3t_{pp(nn)}+1/3t_{np}$, and $T=3/2$ $3N$ states are neglected. This procedure is sufficient for most of the $3N$ scattering observables [31]. Since it is not evident that such an approximate approach is sufficient when the MMI's are included, we performed also calculations where for each partial wave state $|\alpha\rangle$ with isospin $t=1$ both values of the total $3N$ isospin $T=1/2$ and $T=3/2$ were taken into account. In all calculations we considered all basis states $|\alpha\rangle$ with two-nucleon subsystem angular momenta up to $j \leqslant j_{max}=3$. In order to obtain full convergence of the numerical results for elastic scattering and breakup observables, Eq. (1) was solved for total $3N$ angular momenta up to $J=25/2$. Under this condition the maximal number of coupled integral equations, which is equal to the number of possible $|\alpha\rangle$'s, amounts to 62 for the approximate approach and increases to 89 when both values of the total isospin are taken into account.

III. ELASTIC SCATTERING RESULTS

The nucleon scattered off the deuteron can be either a neutron or a proton. Since they have magnetic moments of different sign and magnitude, we performed separate calculations for the pd and nd systems. In both cases the pp (nn) and np nuclear interactions of the AV18 and CD Bonn potentials were used, supplemented by the appropriate MMI's: pp and np for the pd system, and nn and np for the nd system. Comparisons of the theoretical predictions for elastic scattering observables were made between calculations obtained with and without the MMI's included. Among the unpolarized cross section, analyzing powers, spin correlation coefficients, and polarization transfer coefficients, only the vector analyzing powers [$A_y(\theta)$ and $iT_{11}(\theta)$] show a significant influence of the MMI's (see Figs. 1–3). As expected from the different signs of the proton and neutron magnetic moments, the effects of the MMI's have opposite signs for the pd and nd systems.

For the pd system the MMI's raise the maximum value of $A_y(\theta)$ and $iT_{11}(\theta)$ by $\approx4\%$ at $E_n^{lab}=3$ MeV, thus bringing it closer to the experimental pd data, while for the nd system they reduce the maximum of $A_y(\theta)$ and $iT_{11}(\theta)$ by $\approx3\%$, therefore enlarging the discrepancy between theory and data. The magnitude of the MMI effects is energy dependent and decreases with increasing nucleon energy (see Fig. 3). The contribution of the MMI's is thus most significant at low energies. The relative magnitude of the effect is comparable for $A_y(\theta)$ and $iT_{11}(\theta)$ and is roughly independent of the strong NN interaction used in the calculations.

We found that the evaluation of the effects induced by the MMI's does not require partial wave components with total isospin $T=3/2$. Restricting the calculations to the approximate "$\frac{2}{3}$-$\frac{1}{3}$ rule" leads to predictions that deviate from the
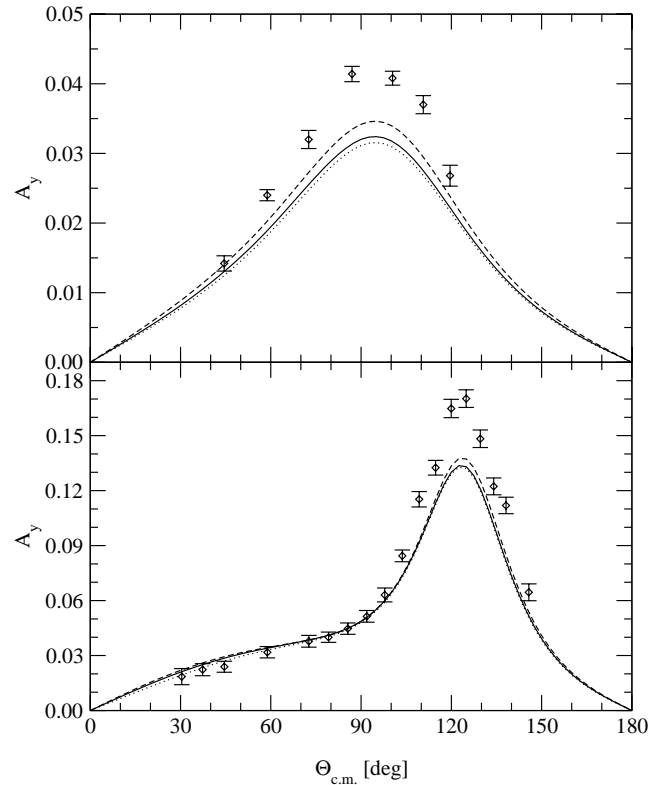

FIG. 1. Effects of MMI's on Nd elastic scattering vector analyzing power $A_y(\theta)$ at $E_n^{lab}=1.9$ MeV (upper part) and $E_n^{lab}=10.0$ MeV (lower part). The solid curve is the CD Bonn potential prediction. Inclusion of MMI's in the pd system leads to the dashed curve and for the nd system to the dotted curve. The nd experimental data are from Refs. [32] (1.9 MeV) and [33] (10.0 MeV).

exact ones by no more than 2%. They exhibit also the same relative changes of observables as the exact calculations when MMI's are included.

Our results once again exemplify the spectacular sensitivity of the low-energy vector analyzing powers to the ^{3}P-wave interactions. In spite of the relative smallness of the MMI contributions to the potential energy of the three nucleons, their effect is amplified by this ^{3}P-wave sensitivity, and they must be taken into account in any final solution to the $A_y(\theta)$ puzzle.

Recent experimental data for the low-energy nd $A_y(\theta)$ ($E_n=1.2$ and 1.9 MeV) revealed a sizable difference with respect to pd data. The difference increases with decreasing center-of-mass energy [32]. This energy dependence was used in Ref. [32] to speculate that the difference between the nd and pd $A_y(\theta)$ data at low energies is due to the MMI's of the three nucleons in the $3N$ continuum. The present work supports qualitatively this conjecture (see Fig. 3). However, a pd calculation including pp Coulomb force is required to quantify it.

IV. BREAKUP RESULTS

The final deuteron breakup state requires five independent kinematical parameters to define it unambiguously. They can
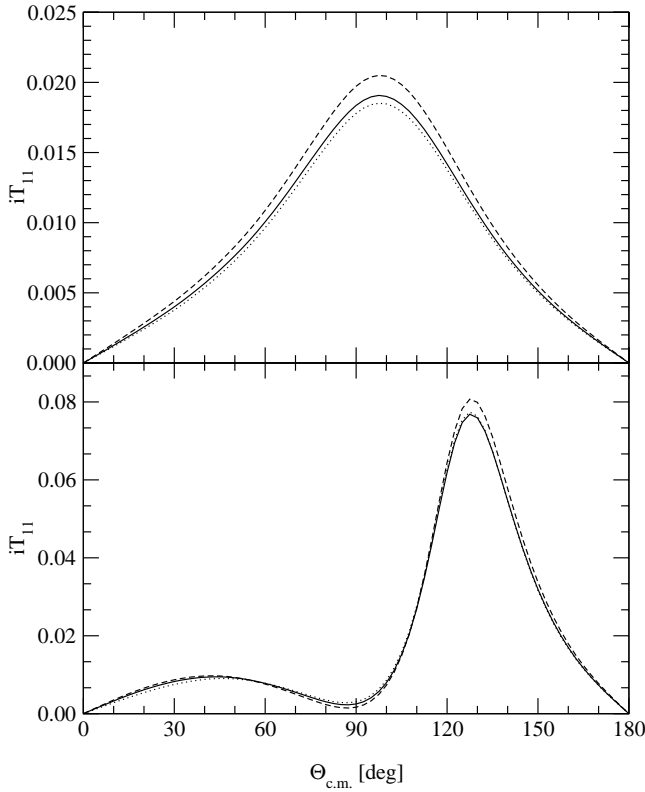
FIG. 2. Effects of MMI's on Nd elastic scattering tensor analyzing power $iT_{11}(\theta)$ at $E_n^{lab} = 1.9$ MeV (upper part) and $E_n^{lab} = 10.0$ MeV (lower part). The solid curve is the CD Bonn potential prediction. Inclusion of MMI's in the pd system leads to the dashed curve and for the nd system to the dotted curve.
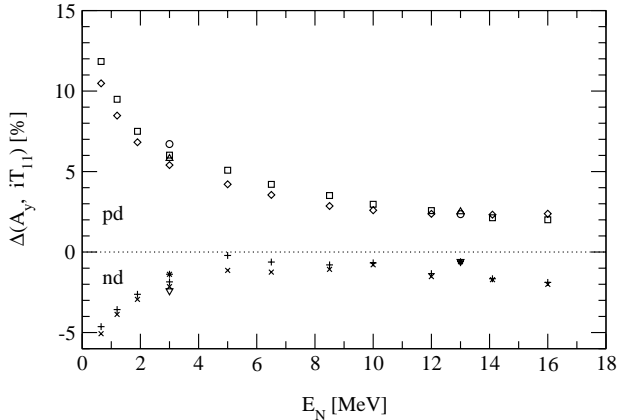

FIG. 3. The energy dependence of the MMI's effect $\Delta = \{[A_y^{(NN)}(iT_{11}) - A_y^{(NN+MMI's)}(iT_{11})]/A_y^{(NN)}(iT_{11})\} \times 100\%$ on vector analyzing powers for elastic Nd scattering at the angle where these observables reach a maximum value. The diamonds and pluses represent Δ predicted by the CD Bonn potential for the pd and nd A_y, respectively. The squares and crosses represent Δ for the pd and nd iT_{11}, respectively. Also, at 3 MeV and 13 MeV the AV18 results are shown [up triangle (star) for the $pd(nd)$ A_y, and circle (down triangle) for the $pd(nd)$ iT_{11}, respectively].

be taken as, e.g., laboratory energies E_1 and E_2 of two outgoing nucleons together with their angles to define the directions of their momenta. In order to locate regions in this five-dimensional breakup phase space with large changes of the cross section due to the MMI's of the nucleons, we applied the projection procedure described in detail in Ref. [11]. The magnitude of the MMI effects on the exclusive breakup cross section $d^5\sigma/d\Omega_1 d\Omega_2 dS$ along the kinematically allowed S curve was defined as

$$\Delta = \left| \frac{\dfrac{d^5\sigma^{(noMMI)}}{d\Omega_1 d\Omega_2 dS} - \dfrac{d^5\sigma^{(MMI)}}{d\Omega_1 d\Omega_2 dS}}{\dfrac{d^5\sigma^{(MMI)}}{d\Omega_1 d\Omega_2 dS}} \right| \times 100\%. \qquad (3)$$

We searched the entire breakup phase space for the distribution of Δ values. For this purpose the phase space was projected onto three subplanes: $\theta_1 - \theta_2$, $\phi_{12} - \theta_2$, and $E_1 - E_2$. Here, θ_1 and θ_2 are the polar angles that together with the azimuthal angles ϕ_1 and ϕ_2 ($\phi_{12} = \phi_1 - \phi_2$) define the directions of the nucleon momenta. The resulting projections of Δ are shown in Fig. 4 at the three incoming proton energies of $E_p^{lab} = 5, 13$, and 65 MeV for the $^2H(p,pp)n$ breakup reaction. The largest changes found for the breakup cross sections reach $\approx 10\%$, and even at 65 MeV there are configurations with non-negligible MMI effects. The largest effects are located mostly in regions of the phase space that are characterized by FSI geometries. In most other parts of the phase space the effects of the MMI's are rather small. In particular, the SST and QFS cross sections are only slightly influenced. According to our calculations, for the QFS configuration the MMI effect depends on the laboratory angles of the quasifree interacting nucleons and it is different for the pp, nn, or np pairs. However, the effects are quite small. At $E_p^{lab} = 13$ MeV they are never larger than 2%. For the SST configuration the effects are smaller than 1%. Changing the c.m. angle between the space-star plane and the beam axis to values different from 90° results in only small changes of the cross section of less than 2% when the MMI's are included.

As stated above, the largest changes of the cross sections of up to $\approx 10\%$ occur for FSI configurations. Their relative magnitude depends on the incoming beam energy and on the production angle of the final-state interacting pair [the (laboratory) angle between the momentum of the FSI pair and the beam axis]. The sign of the effect depends on the type of the final-state interacting pair (see Figs. 5–7). For the np FSI peak the cross section is increased and for the pp (nn) FSI peak it is decreased, according to the increased or decreased attraction caused by the MMI's in the corresponding NN subsystem. The relative changes of the FSI cross sections are comparable for the np and pp FSI peaks, and are a factor of ≈ 2 smaller for the nn FSI peak (see Fig. 5). This factor approximately corresponds to the ratio of the squares of the neutron and proton magnetic moments, $\mu_p^2/\mu_n^2 = 2.13$.

This behavior of the FSI cross sections is of interest in view of recently reported values for the $^1S_0$ nn and np scattering lengths extracted from nd breakup measurements [24,25]. As stated earlier, for the np system both measure-
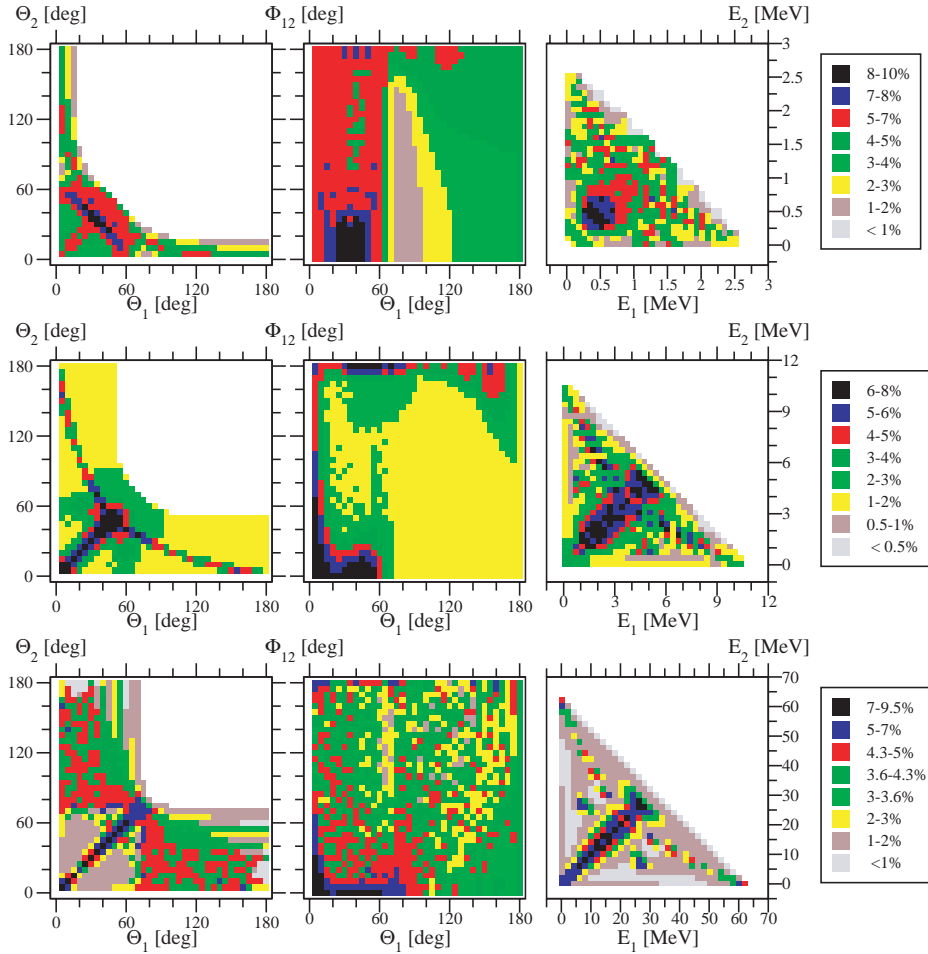
FIG. 4. (Color) Projections of the relative MMI effects Δ on two-dimensional planes for ^{2}H(p,pp)n breakup at $E_p^{lab} = 5, 13$, and 65 MeV (upper row, center row, and bottom row) obtained with the CD Bonn potential. The color scale, adjusted separately for each energy, gives the magnitude of the effect.

ments resulted in comparable values for a_{np}, which agree with the value obtained from free np scattering. However, the reported results for the a_{nn} scattering length are strikingly different. In Fig. 6 we show the nn and np cross sec-
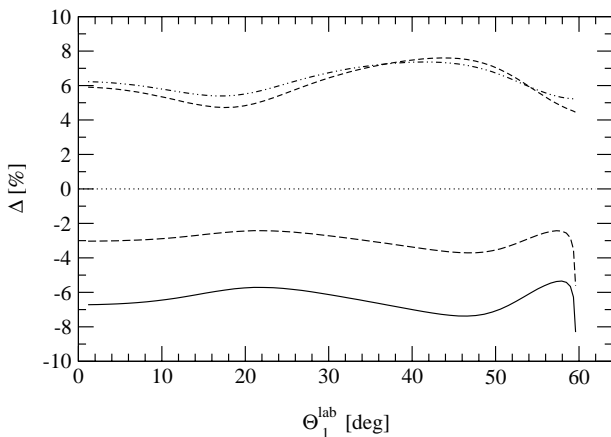

FIG. 5. Effects of MMI's Δ obtained with the CD Bonn potential, on the $E_n^{lab} = 13$ MeV FSI cross sections as a function of the production angle θ_1^{lab}. The solid and long-dashed curves correspond to the pp FSI in the reaction ^{2}H(p,pp)n and the nn FSI in the reaction ^{2}H(n,nn)p, respectively. The effects on the np FSI in these breakup reactions are given by the short-dashed and dashed-double-dotted curves.

tions for the FSI configurations of Ref. [24] and in Fig. 7 for the corresponding configurations of Ref. [25], together with the effects induced by the MMI's on the FSI peaks. It is interesting to note that the theoretical cross sections for the np FSI obtained with MMI's included do not change significantly if the np pair is accompanied by either a nn or pp pair. This effect is slightly dependent on the production angle of the FSI pair (see Fig. 5). This observation, together with our findings about the dependence of the nn FSI peak on the magnitude of the MMI's, indicates a relatively simple mechanism by which the MMI's affect FSI geometries, resulting in a net effect that is dominated by the magnetic moments of the FSI pair.

In view of the non-negligible effects of the MMI's on FSI cross sections found in the present work, one would conclude that the values reported in Refs. [24–26] for the scattering lengths must be corrected for such effects. Based on the sensitivity of the theoretical point-geometry FSI cross sections to specific values of a_{np} and a_{nn} for the geometries of the experiments described in Refs. [24–26], the MMI associated corrections for the a_{np} and a_{nn} scattering lengths are shown in column 3 of Tables I and II, respectively. While the correction to the nn scattering length is rather small, the correction to the np scattering length moves the a_{np} values obtained from the nd breakup reaction away from the free np scattering result by ≈ 1 fm. The corrections given in
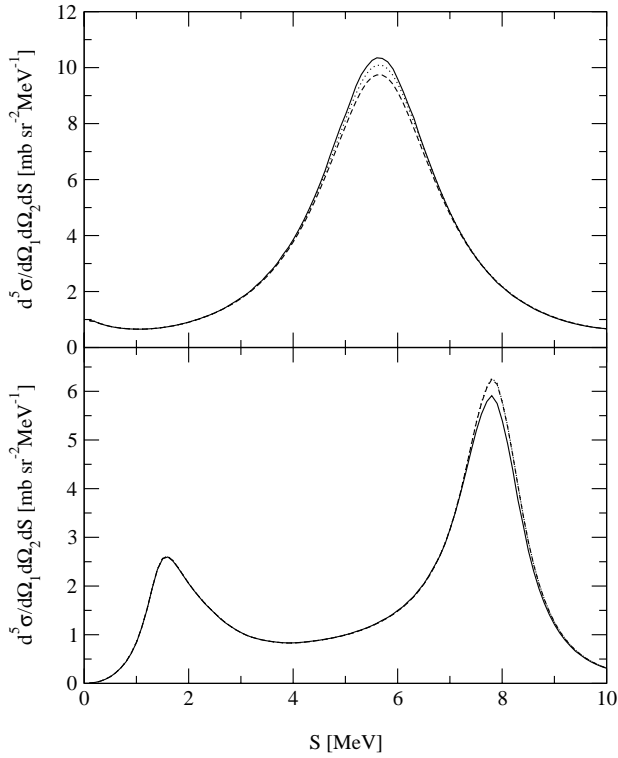
FIG. 6. MMI effects on $E_n^{lab}=13$ MeV nd breakup nn FSI [^{2}H$(n,nn)p$, $\theta_1=\theta_2=28°$, $\phi_{12}=0°$] (upper part) and np FSI [^{2}H$(n,np)n$, $\theta_1=28°,\theta_2=83.5°,\phi_{12}=180°$] (lower part) configurations of Ref. [24]. The CD Bonn potential prediction is given by the solid curve, and the dashed (dotted) curves refer to the calculations with the pp-np (nn-np) MMI's included. Note the overlapping results for the pp-np and nn-np MMI's in the np FSI peak.

FIG. 7. MMI effects in $E_n^{lab}=25.3$ MeV nd breakup nn FSI [^{2}H$(n,np)n$, $\theta_1=55.5°$, $\theta_2=41.15°$, $\phi_{12}=180°$] (upper part) and np FSI [^{2}H$(n,nn)p$, $\theta_1=55.5°,\theta_2=41.15°,\phi_{12}=180°$] (lower part) configurations of Ref. [25]. Descriptions of curves are the same as in Fig. 6. Note the overlapping results for the pp-np and nn-np MMI's in the np FSI peak.

Tables I and II are for point geometry, i.e., they do not include the finite geometry of the experimental setup and the associated energy smearing.

Such sizable corrections, especially for a_{np}, if true, would cast doubt on the accuracy of previous results obtained from the nd breakup reaction. Evidence that this is not the case is shown in Table III. This table contains the effects of including the MMI's with the AV18 and the CD Bonn NN
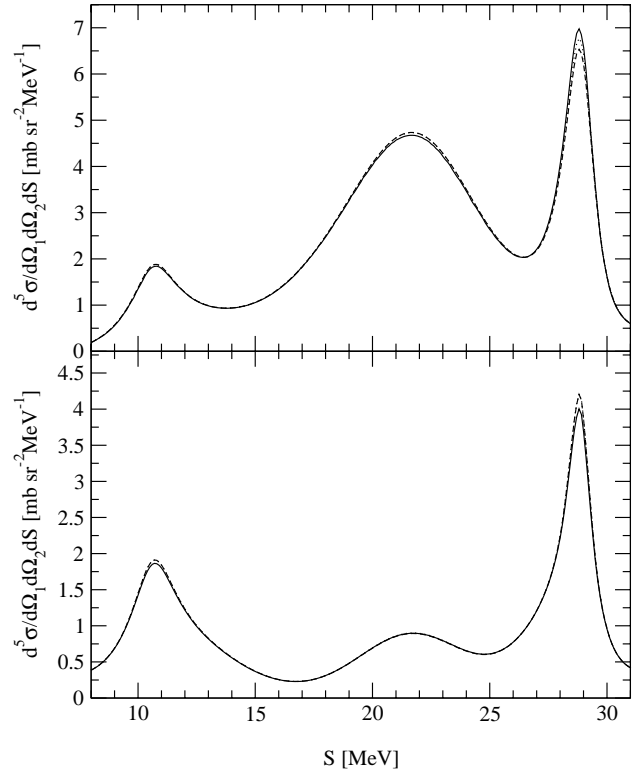
potentials in $2N$ calculations of the $^1S_0$ scattering length. The inclusion of the MMI's increases the magnitude of a_{np}, while for the pp and nn systems, it decreases the magnitude of the scattering lengths. The magnitudes of changes for a_{np} and a_{nn} are nearly equal and opposite in sign to the corrections found for the $3N$ system (see column 3 in Tables I and II and column 5 in Table III). Therefore, the effective corrections, given by their sum, are nearly negligible. The final

TABLE I. The CD Bonn corrections to a_{np} values extracted from np FSI cross sections in nd breakup experiments (see text for explanation of columns).

Configuration	Extracted a_{np} (fm)	MMI corrections (fm)	Corrected a_{np} (fm)
$\theta_1=28°$, $\theta_2=83.5°$, $\phi_{12}=180°$ [a]	-23.7 ± 0.3 [b]	$+0.947$	-23.7 ± 0.3
$\theta_1=35.5°$, $\theta_2=69°$, $\phi_{12}=180°$ [a]	-23.2 ± 0.3 [b]	$+0.985$	-23.2 ± 0.3
$\theta_1=43°$, $\theta_2=55.7°$, $\phi_{12}=180°$ [a]	-23.6 ± 0.3 [b]	$+1.006$	-23.7 ± 0.3
$\theta_1=55.5°$, $\theta_2=41.15°$, $\phi_{12}=180°$ [a]	-23.9 ± 1.0 [c]	$+0.955$	-23.9 ± 1.0
$\theta_1=\theta_2=32°$, $\phi_{12}=0°$ [d]	-24.3 ± 1.1 [e]	$+0.908$	-24.3 ± 1.1

[a]^{2}H$(n,nn)p$.
[b]Reference [24] ($E_n^{lab}=13$ MeV).
[c]Reference [25] ($E_n^{lab}=25.3$ MeV).
[d]^{2}H$(n,np)n$.
[e]Reference [26] ($E_n^{lab}=25$ MeV).

TABLE II. The CD Bonn corrections to a_{nn} values extracted from nn FSI cross sections in nd breakup experiments (see text for explanation of columns).

Configuration	Extracted a_{nn} (fm)	MMI corrections (fm)	Corrected a_{nn} (fm)
$\theta_1=\theta_2=20.5°,\ \phi_{12}=0°$ [a]	-18.9 ± 0.2 [b]	-0.244	-18.8 ± 0.2
$\theta_1=\theta_2=28°,\ \phi_{12}=0°$ [a]	-18.8 ± 0.2 [b]	-0.254	-18.7 ± 0.2
$\theta_1=\theta_2=35.5°,\ \phi_{12}=0°$ [a]	-17.7 ± 0.4 [b]	-0.279	-17.6 ± 0.4
$\theta_1=\theta_2=43°,\ \phi_{12}=0°$ [a]	-18.8 ± 0.4 [b]	-0.306	-18.7 ± 0.4
$\theta_1=55.5°, \theta_2=41.15°,\ \phi_{12}=180°$ [c]	-16.1 ± 0.4 [d]	-0.318	-16.1 ± 0.4
$\theta_1=55.5°, \theta_2=41.15°,\ \phi_{12}=180°$ [c]	-16.2 ± 0.3 [e]	-0.303	-16.1 ± 0.3

[a] ^{2}H$(n,nn)p$.
[b] Reference [24] ($E_n^{lab}=13$ MeV).
[c] ^{2}H$(n,np)n$.
[d] Reference [25] ($E_n^{lab}=25.3$ MeV).
[e] Reference [25] ($E_n^{lab}=16.6$ MeV).

corrected values for a_{np} and a_{nn} are given in column 4 of Tables I and II, respectively. Clearly, the MMI's do not explain the different values for a_{nn} obtained in the measurements of Refs. [24] and [25]. As a side remark one should mention a shortfall of the np $^1S_0$ scattering length used in the CD Bonn potential. It was fitted to the experimental value of a_{np} obtained from free np scattering without taking the MMI into account.

V. SUMMARY AND CONCLUSIONS

We performed an extensive study of effects induced by the magnetic moment interactions of nucleons in the $3N$ continuum. For elastic Nd scattering we found that only the vector analyzing powers show significant changes when the MMI's are included. For the nd system the MMI's increase the discrepancy between calculations and data for $A_y(\theta)$ in the region of the $A_y(\theta)$ maximum, while for the pd system they reduce the discrepancy. The effects for iT_{11} are similar. The relative magnitude of the MMI effects decreases with increasing energy. The recent low-energy nd $A_y(\theta)$ data seem to support the action of the MMI [32]. Our results show that any final solution of the $A_y(\theta)$ puzzle must incorporate the MMI's of the nucleons involved.

For the Nd breakup cross sections the regions where the MMI's are important are restricted to FSI geometries, where changes of the cross sections of up to $\approx10\%$ were found. Such large effects originate from modifications of the $^1S_0$ scattering lengths caused by the MMI's, to which the FSI cross sections are sensitive. Due to these modifications, when extracting scattering length from breakup measurement the MMI's can be neglected in the underlying theory, i.e., the resulting effective corrections are practically negligible. Therefore, the very minor MMI corrections found in the present work do not explain the different values for the $^1S_0$ a_{nn} obtained in recent nd breakup experiments. From the theoretical point of view, the $^1S_0$ scattering lengths a_{nn} and a_{np} can be reliably determined from experimental data, provided the MMI's are treated consistently on the NN and $3N$ levels. If the MMI's are included in only one of these levels, the associated results for the scattering lengths must be corrected appropriately.

In most regions of the phase space Nd breakup cross sections are influenced only slightly by the MMI's. In particular, this is the case for the QFS and SST configurations. Therefore, the MMI's are not responsible for the large differences found between theoretical predictions and data for the nd breakup SST and nn QFS cross sections.

TABLE III. The experimental, AV18, and CD Bonn potential $^1S_0$ scattering lengths, together with MMI corrections (see text for explanation of columns).

System	Experiment (fm)	NN potential (fm)	NN potential with MMI's (fm)	MMI corrections (fm)
np	-23.749 ± 0.008 [a]	AV18: -23.084	-23.863 [b]	-0.779
		CD Bonn: -23.740	-24.685	-0.945
pp	-7.8063 ± 0.0026 [c]	AV18: -17.164	-16.581	$+0.583$
		CD Bonn: -17.466	-16.797	$+0.669$
nn	-18.5 ± 0.4 [d]	AV18: -18.818	-18.487	$+0.331$
		CD Bonn: -18.801	-18.433	$+0.368$

[a] Reference [27].
[b] In [29] V_{C1} (Eq. (12) in Ref. [29]) was included to get experimental a_{np} value.
[c] Reference [34].
[d] Reference [35].

[1] W. Glöckle, H. Witała, D. Hüber, H. Kamada, and J. Golak, Phys. Rep. **274**, 107 (1996), and references therein.

[2] A. Nogga, H. Kamada, and W. Glöckle, Phys. Rev. Lett. **85**, 944 (2000), and references therein.

[3] S.C. Pieper, V.R. Pandharipande, R.B. Wiringa, and J. Carlson, Phys. Rev. C **64**, 014001 (2001).

[4] H. Witała, W. Glöckle, D. Hüber, J. Golak, and H. Kamada, Phys. Rev. Lett. **81**, 1183 (1998).

[5] H. Sakai *et al.*, Phys. Rev. Lett. **84**, 5288 (2000).

[6] R.V. Cadman *et al.*, Phys. Rev. Lett. **86**, 967 (2001).

[7] K. Sekiguchi *et al.*, Phys. Rev. C **65**, 034003 (2002).

[8] R. Bieber *et al.*, Phys. Rev. Lett. **84**, 606 (2000).

[9] K. Ermisch *et al.*, Phys. Rev. Lett. **86**, 5862 (2001).

[10] H. Witała, W. Glöckle, J. Golak, A. Nogga, H. Kamada, R. Skibiński, and J. Kuroś-Żołnierczuk, Phys. Rev. C **63**, 024007 (2001).

[11] J. Kuroś-Żołnierczuk, H. Witała, J. Golak, H. Kamada, A. Nogga, R. Skibiński, and W. Glöckle, Phys. Rev. C **66**, 024003 (2002).

[12] H. Witała, D. Hüber, and W. Glöckle, Phys. Rev. C **49**, R14 (1994).

[13] A. Kievsky, S. Rosati, W. Tornow, and M. Viviani, Nucl. Phys. **A607**, 402 (1996).

[14] W. Tornow and H. Witała, Nucl. Phys. **A637**, 280 (1998).

[15] W. Tornow, A. Kievsky, and H. Witała, Few-Body Syst. **32**, 53 (2002).

[16] H.R. Setze *et al.*, Phys. Lett. B **388**, 229 (1996).

[17] J. Strate *et al.*, Nucl. Phys. **A501**, 51 (1989).

[18] M. Stephan *et al.*, Phys. Rev. C **39**, 2133 (1989).

[19] K. Gebhardt, W. Jäger, C. Jeitner, M. Vitz, E. Finckh, T.N. Frank, Th. Januschke, W. Sandhas, and H. Haberzettl, Nucl. Phys. **A561**, 232 (1993).

[20] S. Churchwell *et al.*, Triangle Universities Nuclear Laboratory Progress Report **XL**, 26 (2001).

[21] S. Churchwell *et al.*, Triangle Universities Nuclear Laboratory Progress Report **XL**, 30 (2001).

[22] W. Lübcke, Ph.D. thesis, University Bochum, 1992.

[23] A. Siepe, J. Deng, V. Huhn, L. Wätzold, Ch. Weber, W. von Witsch, H. Witała, and W. Glöckle, Phys. Rev. C **63**, 014003 (2000).

[24] D.E. González Trotter *et al.*, Phys. Rev. Lett. **83**, 3788 (1999).

[25] V. Huhn, L. Wätzold, Ch. Weber, A. Siepe, W. von Witsch, H. Witała, and W. Glöckle, Phys. Rev. C **63**, 014003 (2000).

[26] J. Deng, A. Siepe, and W. von Witsch, Phys. Rev. C **66**, 047001 (2002).

[27] L. Koester and W. Nistler, Z. Phys. A **272**, 189 (1975).

[28] V.G.J. Stoks, Phys. Rev. C **57**, 445 (1998).

[29] R.B. Wiringa, V.G.J. Stoks, and R. Schiavilla, Phys. Rev. C **51**, 38 (1995).

[30] R. Machleidt, F. Sammarruca, and Y. Song, Phys. Rev. C **53**, R1483 (1996).

[31] H. Witała, W. Glöckle, and H. Kamada, Phys. Rev. C **43**, 1619 (1991).

[32] E.M. Neidel *et al.*, Phys. Lett. B **552**, 29 (2003).

[33] W. Tornow, C.R. Howell, R.C. Byrd, R.S. Pedroni, and R.L. Walter, Phys. Rev. Lett. **49**, 312 (1982).

[34] J.R. Bergervoet, P.C. van Campen, W.A. van der Sanden, and J.J. de Swart, Phys. Rev. C **38**, 15 (1988).

[35] G.F. de Téramond and B. Gabioud, Phys. Rev. C **36**, 691 (1987).